Green Chemistry

COMMUNICATION

View Article Online
View Journal | View Issue

Cite this: *Green Chem.*, 2026, **28**, 7760

Received 3rd February 2026,
Accepted 6th April 2026

DOI: 10.1039/d6gc00740f

rsc.li/greenchem

Plastic waste boosted the plasma-assisted ammonia synthesis process from N_2 and H_2O

Hangtian Hu, Wenping Li,* Hui Zheng, Zheng Li, Aiguo Wang, Zhangxin Chen and Jinguang Hu *

Sustainable ammonia (NH_3) synthesis under moderate conditions, powered by renewable electricity and with reduced CO_2 emissions, is a promising alternative to the energy-intensive Haber–Bosch process. In this work, we developed a non-thermal plasma (NTP) process that simultaneously realizes the synthesis of NH_3 and the upcycling of high-density polyethylene (HDPE) waste with N_2, H_2O, and HDPE as feedstocks. A pronounced synergistic effect on NH_3 yield was observed when HDPE was introduced. HDPE not only acted as a hydrogen donor but also as an oxygen scavenger to suppress H/O recombination, which led to an NH_3 yield increase from 0.7 to 55.9 μmol h^{-1} under low N_2 flow rate conditions, a 78.9-fold increase relative to the case without HDPE. This study offers a novel route for integrating low-carbon NH_3 synthesis with plastic waste valorization, contributing to sustainable energy and waste management strategies.

Green foundation

1. This work demonstrates the potential of waste plastics as an additional hydrogen donor in plasma-assisted ammonia synthesis from N_2 and H_2O, enabling high-yield NH_3 production while simultaneously upgrading waste plastics under ambient conditions. This route offers a potential alternative to the conventional Haber–Bosch process by avoiding external H_2 supply and high-temperature/high-pressure operation.
2. Using high-density polyethylene (HDPE) as a model plastic, packing HDPE substantially enhanced NH_3 formation, increasing the production rate from 0.7 to 55.9 μmol h^{-1} (a 78.9-fold increase). Simultaneously, value-added gaseous byproducts derived from HDPE decomposition, including H_2, CO, CH_4, and C_2H_6, were generated steadily.
3. Future work will optimize reactor design and plastic packing modes to increase productivity and enable scale-up at lower specific energy input. Incorporating catalysts will further direct plastic conversion toward targeted products and improve NH_3 selectivity and energy efficiency.

Introduction

Ammonia (NH_3) is a key feedstock in the production of nitrogen fertilizers and also a promising carbon-free fuel with high hydrogen density.[1,2] Currently, the Haber–Bosch (H–B) process ($N_2 + 3H_2 \leftrightarrow 2NH_3$) dominates ammonia synthesis, which is operated under high pressures (15–35 MPa) and temperatures (350–550 °C), requiring tremendous energy (1%–2% of global energy consumption).[3,4] In addition, H_2 adopted in this process is mainly from natural gas reforming, which causes huge CO_2 emissions, responsible for 1.8% of the global CO_2 total emissions.[4–6] Therefore, alternative technologies need to be explored to synthesize NH_3 under moderate conditions, with less CO_2 emission and driven by renewable electricity.[7]

Given that conventional H_2 production is generally from fossil fuels, replacing the fossil fuel with H_2O as the hydrogen source offers a promising pathway to mitigate carbon emissions. Nowadays, the application of electrocatalytic and photocatalytic methods in the nitrogen reduction reaction ($2N_2 + 6H_2O \rightarrow 4NH_3 + 3O_2$) has been widely investigated.[7–9] However, the NH_3 yield is limited due to the high bond energy of the N≡N bond (941 kJ mol^{-1}), poor N_2 solubility, and low N_2 diffusion coefficient in aqueous solvents. To tackle these issues, non-thermal plasma (NTP) technology has posed a possible solution, which can generate high-energy electrons to activate inert N_2 into more reactive, vibrationally or electronically excited states under mild conditions, facilitating the cleavage of the N≡N bond.[10,11] Dielectric barrier discharge (DBD) plasma, as one of the NTP technologies, is extensively investigated among NTP technologies because of its ability to incor-

Department of Chemical and Petroleum Engineering, University of Calgary, 2500 University Drive, NW, Calgary, Alberta T2N 1N4, Canada.
E-mail: wenping.li@ucalgary.ca, jinguang.hu@ucalgary.ca

porate catalysts or other materials within the reactor while preventing arc discharges from causing damage.

So far, two types of experimental setups have been reported, distinguished by whether H_2O is introduced into the plasma discharge zone. One is a plasma–liquid interface system for NH_3 synthesis developed by Haruyama's group,[12,13] in which N_2 is activated by plasma discharge and subsequently transported to a separate chamber to react with H_2O at the interface. The other is introducing H_2O directly into the discharge zone, enabling a one-step reaction with N_2 to produce NH_3. Toth *et al.*[14] developed a continuous ammonia generation system by co-feeding N_2 gas and atomized H_2O droplets into a DBD reactor, achieving an NH_3 yield of 11 ± 1 μmol h^{-1}. However, a current challenge of H_2O as the hydrogen donor for ammonia synthesis is the low density of generated H species, which tend to recombine with O species, resulting in low energy efficiency and low NH_3 yield.

In parallel, plastic waste upcycling has emerged as an urgent and rapidly growing research direction, driven by the massive accumulation of waste polymers and the need to convert them into value-added chemicals and fuels.[15] In particular, global annual plastic production has increased from about 2 million metric tons (Mt) in 1950 to roughly 400 Mt by 2022.[16] Recently, NTP has also been explored as a promising platform for plastic waste upcycling to hydrogen. For example, Trelles's group[17] developed ambient-pressure reactors based on transferred-arc and gliding-arc discharges to convert low-density polyethylene (LDPE) into hydrogen, achieving maximum H_2 productions of 0.33 and 0.42 mmol g^{-1} LDPE, respectively.

In this work, to overcome the intrinsic limitation of H_2O-based plasma for ammonia synthesis and boost the ammonia yield, we creatively introduced plastic waste into the DBD reactor, by providing a second hydrogen donor and consuming oxygen generated from H_2O decomposition to generate more H species. In this novel process, NH_3 synthesis can be concurrently coupled with plastic waste valorization within a single reactor. High-density polyethylene (HDPE) was selected as the model plastic to realize and explore this plastic-boosted ammonia synthesis process, owing to its large market share, high hydrogen content (high H/C ratio), and the absence of oxygen in its polymer backbone. Control experiments were conducted to elucidate the effects of HDPE packing amount, H_2O concentration, flow rate, and specific energy input (SEI) on the yields of NH_3 and gaseous products. Based on product analysis and characterization of fresh and spent HDPE, a plausible reaction mechanism was proposed.

Experimental section

Herein, we developed an integrated DBD system to simultaneously realize NH_3 synthesis and HDPE upcycling under mild conditions (Fig. 1). The setup comprises a gas supply unit, an AC high-voltage (HV) power supply (High Voltage Plasma Generator G2000, Redline Technologies), a DBD reactor, a product collection unit, a micro-gas chromatograph (990 Micro GC System, Agilent), and a UV-Vis spectrophotometer (Clarus 590, PerkinElmer). Humidity control of the inlet N_2 was achieved using two mass flow controllers (FMA-2617A, OMEGA) in conjunction with a water bubbler. The total N_2 flow rate was varied between 10 and 1000 SCCM, and the H_2O vapor concentration was expressed as the relative saturation percentage at ambient temperature (21 °C). The DBD reactor consisted of a quartz tube (200 mm length; 8 mm inner diameter; 10 mm outer diameter) with a centrally positioned stainless steel rod (4 mm diameter) serving as the HV electrode. The discharge gap was fixed at 2 mm. A stainless-steel mesh wrapped around the outer surface of the quartz tube acted as the grounded electrode, allowing adjustment of the discharge length from 20 to 80 mm. The input power used in this work refers to the applied plasma generator power, rather

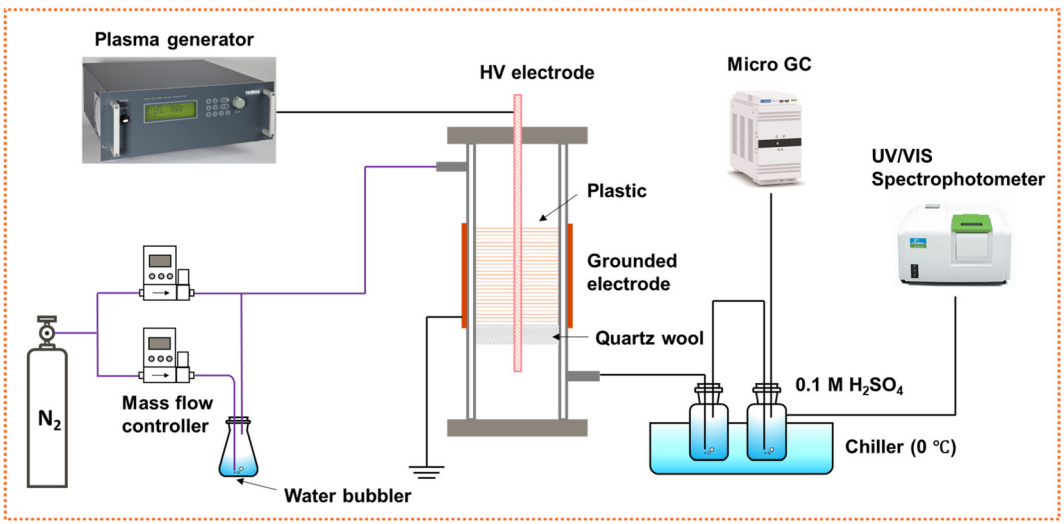

Fig. 1 Schematic of the experimental setup for plasma-assisted NH_3 synthesis from N_2, H_2O and plastic waste.

than the directly measured discharge power. HDPE waste, sourced from discarded milk bottles, was cut into rectangular pieces (10 × 4 mm) and positioned in the discharge zone. Two bottles containing 0.1 M sulfuric acid were adopted to trap NH_3 from the outlet gas, which was subsequently analyzed by micro GC. The concentration of NH_3 in the aqueous sulfuric acid solution was detected by UV-Vis spectrophotometry. The liquid products retained in the DBD reactor were extracted with chloroform and subsequently characterized by ^1H NMR (400 MHz Avance III Spectrometer, Bruker) and GC-MS (Agilent 6890).

Results and discussion

We first verified the boost effect of the HDPE packing on NH_3 yields under different reactant feeding and packing conditions, as shown in Fig. 2a and Table S1. No NH_3 was detected when Ar was used as the reactant gas. Introducing H_2O produced only a trace amount of NH_3, whereas using HDPE led to a much higher NH_3 yield, highlighting the strong capability of HDPE to serve as a hydrogen donor. Notably, co-feeding H_2O and HDPE resulted in a significant increase in NH_3 yield that exceeded the sum of the yields obtained when each component was fed individually, indicating a synergistic effect between H_2O activation and HDPE decomposition and underscoring the potential of this coupled system for enhanced NH_3 production. The effect of HDPE packing amount on NH_3 and gaseous co-product yields was further investigated. As shown in Fig. 2b and c, the absence of HDPE led to extremely low NH_3 and H_2 yields, only 0.7 and 21.2 μmol h^{-1}, respectively. However, upon introducing HDPE into the plasma discharge zone, both NH_3 and H_2 product yields showed pronounced enhancement, and reached 55.9 μmol h^{-1} and 1282.7 μmol h^{-1} at 1000 mg HDPE packing amount, respectively. This confirms the role of HDPE as a critical hydrogen donor. In addition, as the HDPE packing amount increased from 250 to 1000 mg, the NH_3 yield increased from 4.86 to 55.9 μmol h^{-1}, while the energy efficiency improved from 2.07 to 23.76 mg kWh^{-1}. The elevated H_2 yield indicates greater H radical availability in the plasma, thereby promoting N–H bond formation and significantly boosting NH_3 synthesis.[18] Approximately 3–6 wt% of the HDPE decomposed during 1 h plasma discharge, generating H_2, CO (303.9 μmol h^{-1}), CH_4 (191.3 μmol h^{-1}), C_2H_4 (13.0 μmol h^{-1}) and C_2H_6 (41.5 μmol h^{-1}) as primary gaseous byproducts (Fig. 2c and

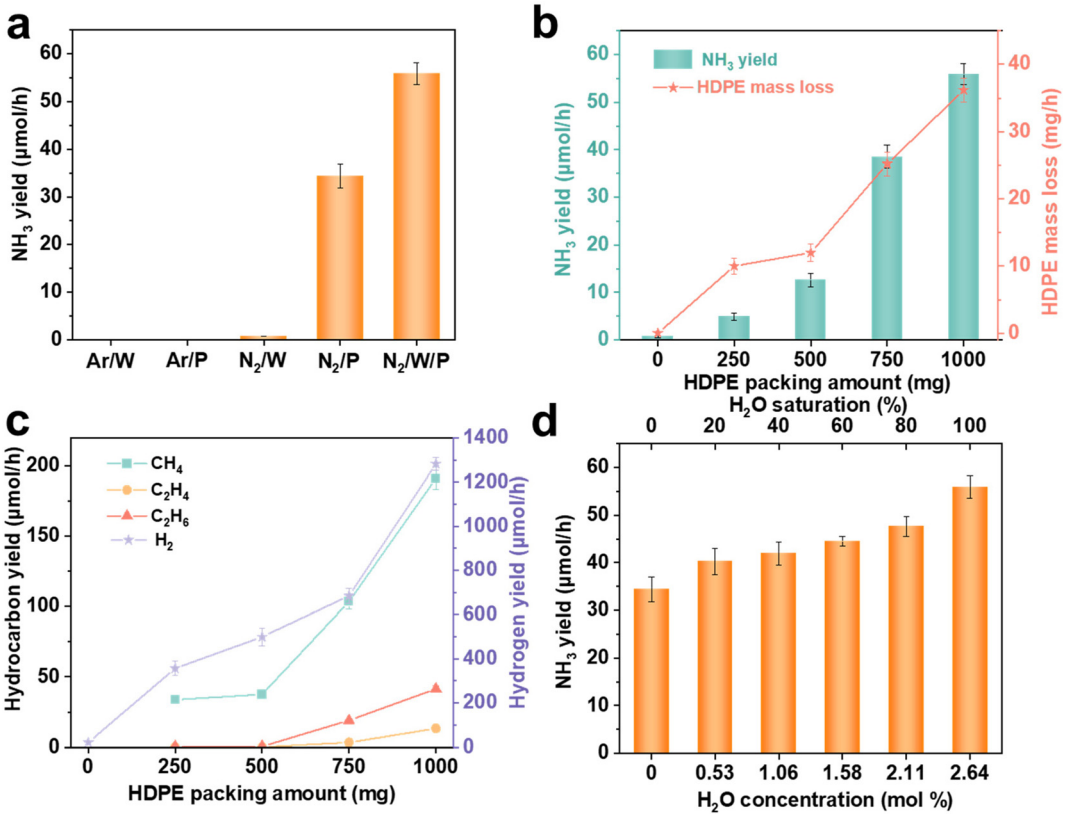

Fig. 2 (a) Comparison of NH_3 yield under different feeding gas and packing conditions: argon with water (Ar/W), argon with HDPE packing (Ar/P), N_2 with water (N_2/W), N_2 with HDPE packing (N_2/P), and N_2 with water and HDPE packing (N_2/W/P) (flow rate: 10 SCCM; 2.64 mol% H_2O; input power: 40 W). Effect of HDPE packing amount on (b) NH_3 yield and HDPE mass loss, and on (c) gaseous product yields (partial packing; feeding gas: N_2 + H_2O; flow rate: 10 SCCM; 2.64 mol% H_2O; input power: 40 W). (d) Effect of H_2O concentration in the N_2 feed on NH_3 yield (full packing; feeding gas: N_2 + H_2O; flow rate: 10 SCCM; input power: 40 W).

Fig. S1). It should be noted that HDPE decomposition was highly sensitive to the packing configuration. In this work, two configurations, full packing and partial packing, were employed (Fig. S2). The key difference between these two modes is whether the discharge length changes with the packing amount. In the partial packing mode, the discharge length was fixed at 80 mm, while HDPE packing amounts of 250, 500, 750, and 1000 mg corresponded to 25%, 50%, 75%, and 100% occupancy of the discharge volume, respectively. Under partial packing mode, HDPE decomposition remained weak within low discharge-volume occupancy. At occupancies ≤50% (≤500 mg), inefficient filamentary discharges in the non-packing zone consumed significant energy but contributed negligibly to HDPE decomposition.[19,20] This was evidenced by a trace amount of C_2H_4/C_2H_6 production and stable CH_4 yields despite increased HDPE packing amount (250 → 500 mg) (Fig. 2d). Further validation *via* reactor performance comparison (Fig. S3 and S4) revealed that full packing enhanced NH_3 yields by 293%, 120%, and 27% relative to partial packing at 25%, 50%, and 75% occupancy, respectively, with the same HDPE packing amount. Moreover, H_2 and gaseous product yields plateaued as the HDPE loading amount increased from 500 to 1000 mg HDPE under full packing conditions (Fig. S5), indicating comparable decomposition rates at ≥50% occupancy. To distinguish the generic packed-bed effect from the specific role of HDPE, a control experiment using glass beads as an inert packing material was conducted. As shown in Fig. S6, glass beads resulted in only a slight increase in NH_3 yield compared with the empty reactor, whereas HDPE packing led to a dramatic enhancement. This result suggests that the improvement is not merely due to the presence of a packed bed but is closely related to the unique role of HDPE in the plasma-assisted reaction system.

The influence of H_2O concentration on NH_3 synthesis was further investigated through control experiments. As depicted in Fig. 2d and Fig. S7, increasing the H_2O concentration from 0 to 2.64 mol% (H_2O saturation percentage from 0 to 100%) improved the NH_3 yield from 34.3 to 55.9 μmol h^{-1} and the H_2 yield from 810.6 to 1280.7 μmol h^{-1}, demonstrating that H_2O also served as an effective hydrogen donor for NH_3 and H_2 formation when HDPE was packed. In addition, increasing the H_2O concentration revealed a clear synergy between H_2O dissociation and HDPE decomposition to H species. In the absence of HDPE packing, the H_2 yield remained relatively low (Fig. 2c), only 21.2 μmol h^{-1}, indicating weak H_2O dissociation. By contrast, under HDPE packing conditions, raising the H_2O concentration substantially increased the H_2 yield (Fig. S7), suggesting that the presence of HDPE promotes H_2O activation and amplifies the H_2O concentration dependence of H_2 production. This enhanced dissociation implies that HDPE could function as an oxygen scavenger, capturing oxygen atoms liberated during H_2O cleavage (verified further below) and thereby preventing H/O recombination. Furthermore, the presence of H_2O in the DBD reactor led to the formation of CO and NO_x gases. CO is formed *via* coupling between carbonaceous fragments from HDPE and oxygen species from H_2O dissociation under plasma discharge, whereas NO_x arises from oxidation of nitrogen-centered radicals formed during the reaction. NO_x was captured in two tandem sulfuric acid bottles, yielding aqueous nitrate and nitrite. Both the CO yield and the combined nitrate/nitrite yields increased monotonically with H_2O concentration (Fig. S7 and S8). Limited CO_2 was generated upon H_2O introduction, with the yield increasing from 0 to 21.0 μmol h^{-1} as the H_2O concentration rose from 0 to 2.64 mol%. Temperature monitoring of the discharge region further showed that, under the same input power, the measured discharge region temperatures were essentially identical for the empty-tube and HDPE-packed reactors, and no obvious difference in the discharge region temperature was observed within the investigated range with varying H_2O content or HDPE packing amount (Fig. S9).

The influence of N_2 flow rate and SEI on NH_3 production was systematically investigated, with SEI controlled *via* input voltage adjustment. As shown in Fig. 3a, increasing the N_2 flow rate enhanced NH_3 yields in both empty and HDPE packing reactors. This trend is attributed to the reduced gas residence time at higher flow rates, which mitigates equilibrium constraints on NH_3 formation by suppressing its reverse dissociation.[21] At 10 SCCM, HDPE packing increased the NH_3 yield from 0.7 to 55.9 μmol h^{-1}, representing a pronounced 78.9-fold enhancement, while the energy efficiency increased from 0.30 to 23.76 mg kWh^{-1}. Even at 1000 SCCM (GHSV ≈ 20 000 h^{-1}), HDPE packing still delivered a 3.7-fold increase, increasing the NH_3 yield from 26.2 to 92.3 μmol h^{-1} and the energy efficiency from 11.1 to 39.2 mg kWh^{-1}. The weakened HDPE packing benefit at high gas flow rates is attributed to the dilution effect of high flow rates, where the residence time shortens and reactive H species are diluted and swept out more rapidly, thereby weakening HDPE's role as an effective hydrogen donor. For the SEI experiments, the N_2 flow rate was fixed at 10 SCCM. Raising the SEI from 240 to 306 kJ L^{-1} increased the NH_3 yield from 57.6 to 97.2 μmol h^{-1} (Fig. 3b). This enhancement likely arises from the stronger plasma-induced fragmentation and activation of gaseous reactants and HDPE at higher SEI, leading to higher densities of reactive species and more productive collisions for NH_3 formation.[19,20] The energy efficiency also showed a modest increase with SEI, suggesting that the additional energy input was still effectively utilized for the target reaction within the investigated range. In contrast, when SEI was varied by changing the gas flow rate under fixed applied input power (Fig. S10), different trends were observed, indicating that the apparent SEI effect is coupled with the experimental parameter used to vary it. In particular, varying the flow rate also changes the gas throughput, the residence time in the discharge zone, and the capture behavior of NH_3 in the downstream acid solution. A comparison table has been added to summarize NH_3 yield and energy efficiency for representative reports in related fields (Table S2). The table shows that, although plasma routes can achieve relatively high NH_3 yields among electrified NH_3 synthesis approaches, their energy consumption remains substantially

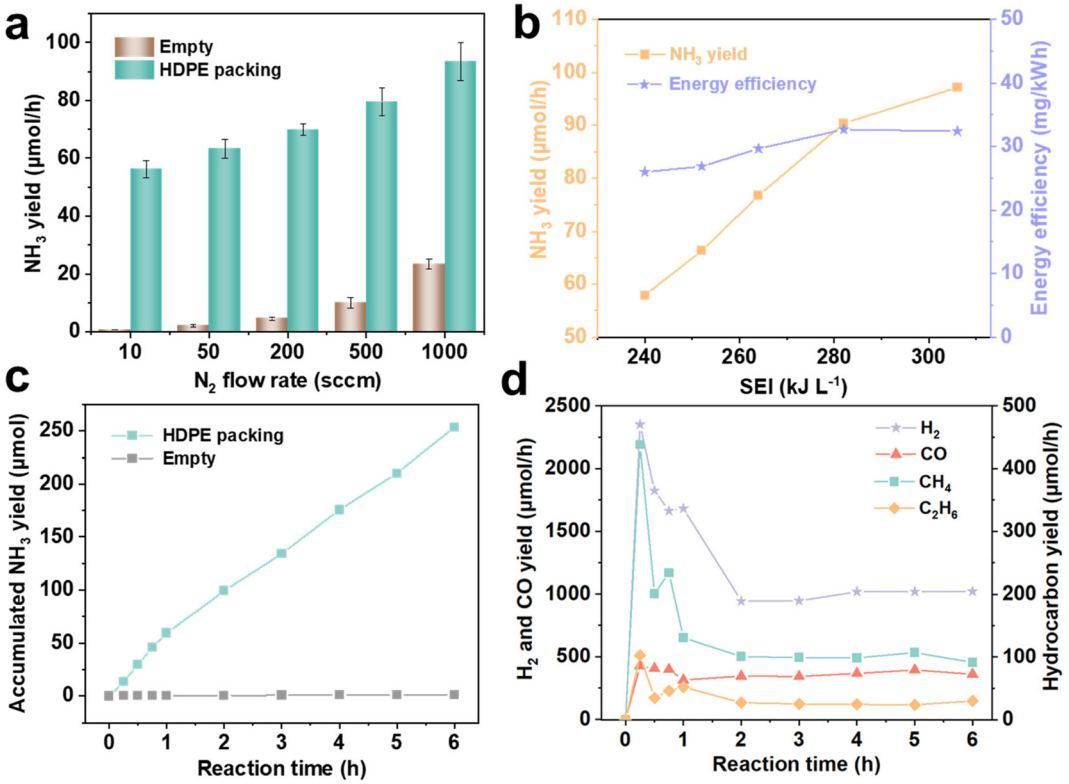

Fig. 3 (a) Comparison of NH_3 yield between a full packing HDPE (1000 mg) reactor and an empty reactor under different N_2 flow rates (full packing; feeding gas: N_2 + H_2O; 2.64 mol% H_2O; input power: 40 W). (b) Effect of SEI on NH_3 yield and energy efficiency (full packing; feeding gas: N_2 + H_2O; flow rate: 10 SCCM; 2.64 mol% H_2O; HDPE packing mass: 1000 mg; input power increased from 40 to 51 W). (c) Comparison of NH_3 yield between a full packing HDPE (1000 mg) reactor and an empty reactor during a 6 h stability test. (d) Gaseous product yields for a full packing HDPE (1000 mg) reactor during a 6 h stability test (full packing; feeding gas: N_2 + H_2O; flow rate: 10 SCCM; 2.64 mol% H_2O; HDPE packing mass: 1000 mg; input power: 40 W).

higher than that of several direct electrocatalytic or Li-mediated routes. Therefore, further progress toward industrially relevant plasma NH_3 synthesis requires simultaneous improvement in both NH_3 production rate and energy efficiency.

As shown in Fig. 3c and d, the stability of the plasma-assisted NH_3 synthesis process from N_2, H_2O and HDPE was assessed over 6 h. HDPE was fully packed into the reactor. The feeding gas consisted of N_2 saturated with 2.64 mol% H_2O at a flow rate of 10 SCCM, and the input power was 40 W. During the experiments, plasma stability and steady-state operation were assessed by monitoring the temperature of the plasma zone with an infrared thermal camera (TOPDON TC002C), the concentration of gaseous byproducts detected by micro-GC, and the current reading displayed on the plasma generator. Throughout the stability test, NH_3 continued to accumulate at a comparable rate over time. Notably, the elevated yields of gaseous products within the first hour suggest more active HDPE decomposition, as carbonaceous gas yields reflect the extent of polymer fragmentation. This is attributed to the direct exposure of fresh HDPE surfaces to reactive plasma species, which promotes rapid chain scission. Subsequently, gradual surface oxidation introduces oxygen-containing functional groups that partially passivate the polymer surface and reduce the accessibility of fresh chains to reactive species. As a result, the yields of NH_3 and gaseous byproducts decreased after the first hour and then remained stable over the subsequent five hours. Additionally, gaseous products were generated steadily over the subsequent five hours, predominantly H_2, CO, CH_4, and C_2H_6, with production rates of 1020.3, 359.6, 91.3 and 29.7 μmol h^{-1}, respectively.

Analysis of the liquid products retained in the DBD reactor by ^1H NMR (Fig. 4a) revealed alkyl chains as the dominant constituents, indicating that these liquids likely originated from chain scission of HDPE. As the reaction time increased from 30 to 60 minutes, both the number and intensity of alkyl chain signals significantly increased. GC-MS analysis was then employed to determine the carbon chain length distribution (Fig. 4b). The results demonstrated a rise in the relative abundance of C_4–C_8 products with extended reaction time, consistent with progressive fragmentation of longer hydrocarbon chains. In addition, carbon-balance and hydrogen-balance analyses were performed for the 1 h reaction under the full-packing condition (Tables S3 and S4). The carbon balance gave an error of 5.52%, while the hydrogen balance gave an error of 8.18%, indicating reasonably good closure of the main

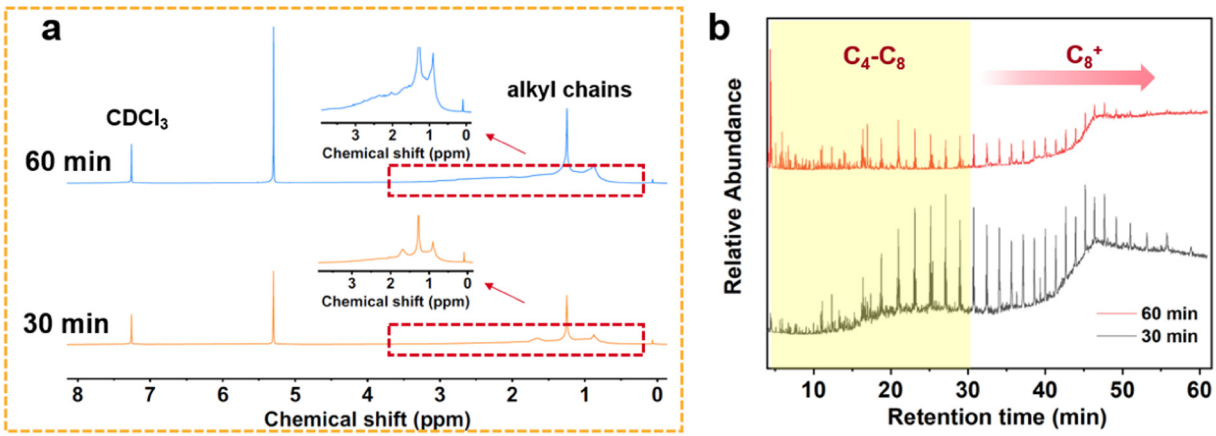

Fig. 4 Liquid products from HDPE treated with plasma for 30 and 60 min, characterized by (a) ^{1}H NMR and (b) GC-MS.

measured products under the present reaction conditions. Moreover, the NH_3 yield increased with increasing HDPE mass loss (Fig. S11), suggesting that NH_3 formation is associated with HDPE consumption. At the same time, since only a small fraction of the available hydrogen is ultimately incorporated into NH_3, HDPE should be regarded as an auxiliary hydrogen donor rather than a highly selective hydrogen source for NH_3 formation.

An HDPE-derived solid was also analyzed to elucidate the interactions among HDPE, N_2, and H_2O. SEM imaging revealed the formation of numerous surface defects on HDPE after plasma treatment, indicating that the plasma-induced decomposition was predominantly a surface process rather than bulk degradation (Fig. 5a and b). FTIR analysis was performed to track surface functional group evolution during a 1 h reaction. As shown in Fig. 5c, characteristic peaks corresponding to C–H stretching (3000–2800 cm^{-1}), methylene bending (1462 cm^{-1}), and methylene rocking vibration (720 cm^{-1}) were present throughout the reaction.[22,23] A gradual decrease in peak intensities with time indicated C–H

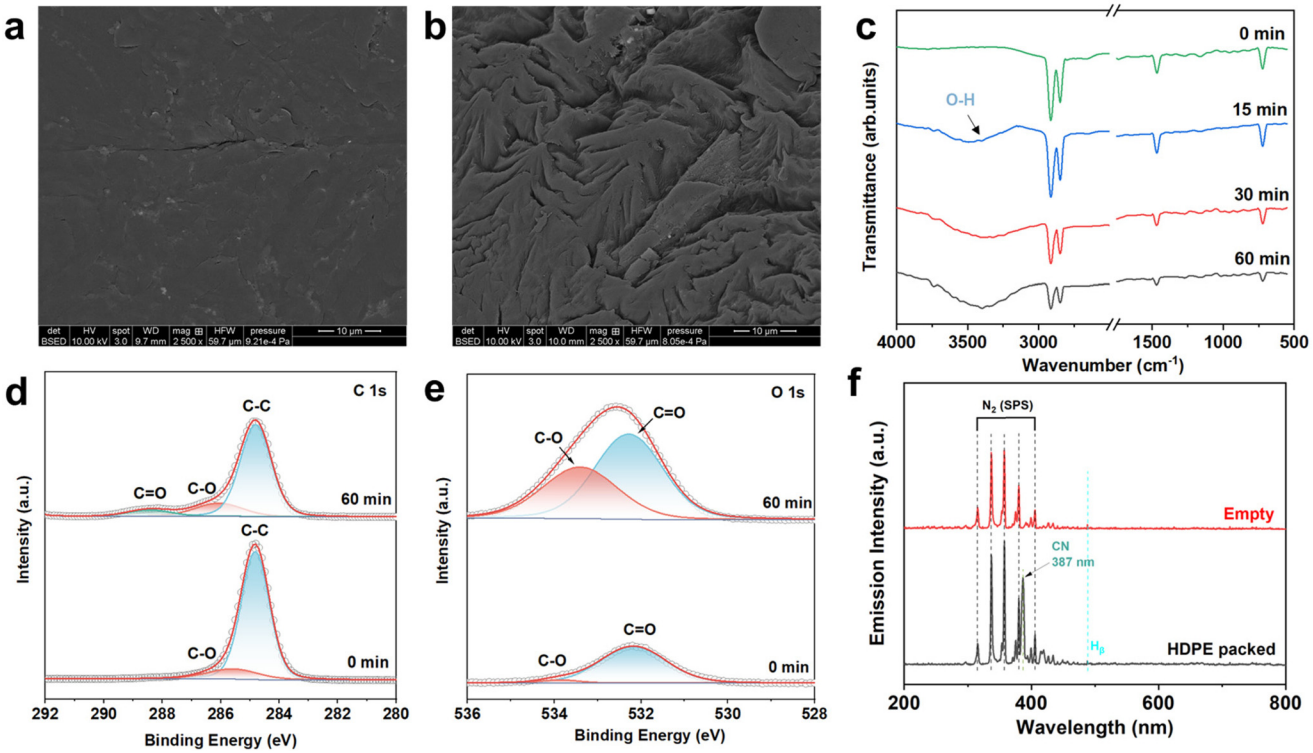

Fig. 5 SEM micrographs of HDPE (a) before and (b) after plasma treatment. Chemical structure analysis of HDPE after different plasma treatment times: (c) FTIR spectra, (d) C 1s XPS spectra, and (e) O 1s XPS spectra. (f) OES comparison of N_2–H_2O plasma between a full packing HDPE (1000 mg) reactor and an empty reactor.

and C–C bond cleavage in HDPE.[24] A new absorption band at 3440 cm^{-1}, attributable to –OH groups, emerged and intensified over time, suggesting adsorption of O or OH species originating from H_2O dissociation. XPS analysis was conducted to further examine surface chemical changes before and after plasma exposure (Fig. 5d and e). The O 1s spectrum of the fresh HDPE indicated the presence of oxygen-containing species (mainly C═O), likely from surface oxidation or oxygen-containing additives. After 60 min of plasma treatment, the relative intensities of C–O (533.2 eV) and C═O (532.3 eV) peaks increased markedly,[23] confirming the adsorption of O atoms generated from H_2O dissociation. The C 1s spectrum showed a decline in the C–C peak, and the overall C/O ratio decreased from 16.9 to 4.2. These results further indicate that HDPE not only serves as a hydrogen source but also acts as an oxygen scavenger in the discharge environment, thereby promoting H_2O dissociation and suppressing the combination of O atoms with N or H atoms, both contributing to enhanced NH_3 yield.

Operando optical emission spectroscopy (OES, AvaSpec-ULS4096CL-EVO, AVANTES) was employed to identify active plasma species. As shown in Fig. 5f, the OES spectra of both the empty-tube and HDPE-packed discharges are dominated by the second positive system (SPS) of N_2, corresponding to the $C^3\Pi_u \rightarrow B^3\Pi_g$ transition, indicating the presence of electronically excited N_2 species in the plasma. Compared with the empty-tube case, the HDPE-packed discharge exhibits substantially enhanced emission intensity, suggesting a stronger discharge and higher population of excited species. A distinct CN emission near 387 nm is observed only for the plastic-packed case, indicating the formation of carbon-containing plasma species arising from the interaction between the discharge and HDPE (Fig. S12).[25] In addition, H_β emission is also observed, consistent with the generation of hydrogen-containing reactive species in the plasma.[26] Overall, these results confirm that packing HDPE significantly alters the discharge chemistry and promotes the formation of a richer pool of excited nitrogen, hydrogen, and carbon-containing species relevant to NH_3 synthesis and concurrent plastic conversion.

Based on the results described above, the reaction mechanism for NH_3 synthesis and the formation of other gaseous and liquid byproducts is proposed, as illustrated in Fig. 6. During plasma discharge, high-energy electrons induce the scission of HDPE chains, generating small radicals, primarily $H^\bullet$ and $^\bullet CH_3$, as well as liquid alkanes, which can subsequently decompose into smaller radicals. These reactive species can combine with each other to generate gaseous products such as H_2, CH_4, C_2H_6, and C_2H_4. Concurrently, N_2 molecules are excited to N_2^+ electronic states, which can react with H radicals to form NH_3. Upon introducing H_2O into the reactor, it undergoes electron-impact dissociation, generating additional H radicals as well as O-containing species. There are three main pathways for consuming O species. First, O species can be adsorbed on the HDPE surface, thereby suppressing H/O recombination and significantly increasing the concentration of H radicals in the plasma. Second, part of the O species can

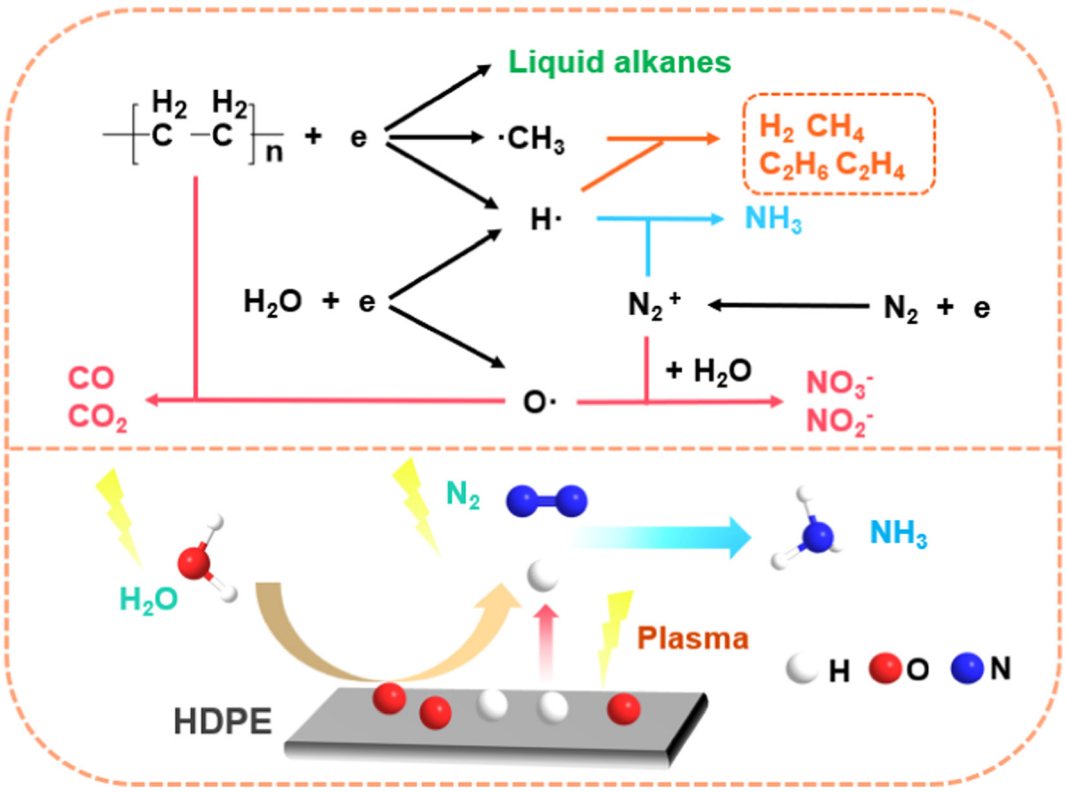

Fig. 6 Proposed reaction mechanism for NH_3 synthesis in a DBD plasma reactor packed with HDPE.

react with carbon fragments derived from HDPE, forming CO and CO_2. Third, a fraction of the O radicals may also react with N_2^+ to produce NO_x species (absorbed in aqueous solution, generating NO_3^- and NO_2^-), although their yield remains limited.

Conclusions

In conclusion, for the first time, plastic waste was introduced into the NTP-assisted ammonia synthesis system from H_2O and N_2 under ambient conditions without external H_2 supply or high-temperature/pressure operation, which boosted ammonia yield and simultaneously enabled waste plastic upcycling. Experimental data indicated that packing HDPE into the reactor greatly increased the NH_3 production rate from 0.7 to 55.9 μmol h^{-1} under flow rate conditions, achieving a 78.9-fold enhancement, while the energy efficiency increased from 0.25 to 20.22 mg kWh^{-1}. In addition, as the HDPE packing amount increased from 250 to 1000 mg, the NH_3 yield increased from 4.86 to 55.9 μmol h^{-1}, while the energy efficiency improved from 2.07 to 20.22 mg kWh^{-1}. The discharge was most intense when the reactor was fully packed with HDPE. In addition to NH_3, gaseous products were generated simultaneously, mainly H_2, CO, CH_4, and C_2H_6, with stable production rates of 1020.3, 359.6, 91.3 and 29.7 μmol h^{-1}, respectively. Beyond serving as a hydrogen donor, HDPE also functioned as an oxygen scavenger, capturing O radicals in the plasma and thereby suppressing undesired H/O recombination, further promoting the dissociation of H_2O. Future work on NH_3 yield enhancement will be focused on optimizing reactor design to promote HDPE decomposition, as well as incorporating catalysts to selectively adsorb N and H radicals.

Conflicts of interest

The authors declare that they have no known competing financial interests or personal relationships that could have appeared to influence the work reported in this paper.

Data availability

The data supporting this article have been included as part of the supplementary information (SI). Supplementary information: supplementary experiments. See DOI: https://doi.org/10.1039/d6gc00740f.

References

1 R. F. Service, *Science*, 2014, **345**, 610.
2 K. M. Bryan, H. R. Suryanto, J. Choi, R. Y. Hodgetts, H.-L. Du, J. M. Bakker, C. S. M. Kang, P. V. Cherepanov, A. N. Simonov and D. R. MacFarlane, *Science*, 2021, **372**, 1187–1191.
3 X. Zhang, R. Su, J. Li, L. Huang, W. Yang, K. Chingin, R. Balabin, J. Wang, X. Zhang, W. Zhu, K. Huang, S. Feng and H. Chen, *Nat. Commun.*, 2024, **15**, 1535.
4 I. Muzammil, Y.-N. Kim, H. Kang, D. K. Dinh, S. Choi, C. Jung, Y.-H. Song, E. Kim, J. M. Kim and D. H. Lee, *ACS Energy Lett.*, 2021, **6**, 3004–3010.
5 L. R. Winter and J. G. Chen, *Joule*, 2021, **5**, 300–315.
6 K. Wang, D. Smith and Y. Zheng, *Carbon Resour. Convers.*, 2018, **1**, 2–31.
7 G. Qing, R. Ghazfar, S. T. Jackowski, F. Habibzadeh, M. M. Ashtiani, C. P. Chen, M. R. Smith 3rd and T. W. Hamann, *Chem. Rev.*, 2020, **120**, 5437–5516.
8 J. Zhao, G. Ren and X. Meng, *Nano Energy*, 2024, **130**, 110109.
9 L. Shi, Y. Yin, S. Wang and H. Sun, *ACS Catal.*, 2020, **10**, 6870–6899.
10 A. Bogaerts and E. C. Neyts, *ACS Energy Lett.*, 2018, **3**, 1013–1027.
11 P. Mehta, P. Barboun, D. B. Go, J. C. Hicks and W. F. Schneider, *ACS Energy Lett.*, 2019, **4**, 1115–1133.
12 T. Haruyama, T. Namise, N. Shimoshimizu, S. Uemura, Y. Takatsuji, M. Hino, R. Yamasaki, T. Kamachi and M. Kohno, *Green Chem.*, 2016, **18**, 4536–4541.
13 T. Sakakura, S. Uemura, M. Hino, S. Kiyomatsu, Y. Takatsuji, R. Yamasaki, M. Morimoto and T. Haruyama, *Green Chem.*, 2018, **20**, 627–633.
14 J. R. Toth, N. H. Abuyazid, D. J. Lacks, J. N. Renner and R. M. Sankaran, *ACS Sustainable Chem. Eng.*, 2020, **8**, 14845–14854.
15 L. Lebreton and A. Andrady, *Humanit. Soc. Sci. Commun.*, 2019, **5**, 1–11.
16 K. Houssini, J. Li and Q. Tan, *Commun. Earth Environ.*, 2025, **6**, 257.
17 B. Tabu, K. Akers, P. Yu, M. Baghirzade, E. Brack, C. Drew, J. H. Mack, H.-W. Wong and J. P. Trelles, *Int. J. Hydrogen Energy*, 2022, **47**, 39743–39757.
18 K. van 't Veer, Y. Engelmann, F. Reniers and A. Bogaerts, *J. Phys. Chem. C*, 2020, **124**, 22871–22883.
19 Y. Wang, M. Craven, X. Yu, J. Ding, P. Bryant, J. Huang and X. Tu, *ACS Catal.*, 2019, **9**, 10780–10793.
20 J. Feng, P. Ning, K. Li, X. Sun, C. Wang, L. Jia and M. Fan, *ACS Sustainable Chem. Eng.*, 2023, **11**, 804–814.
21 T. Zhang, R. Zhou, S. Zhang, R. Zhou, J. Ding, F. Li, J. Hong, L. Dou, T. Shao, A. B. Murphy, K. Ostrikov and P. J. Cullen, *Energy Environ. Mater.*, 2022, **6**, e12344.
22 S. H. Lee, J. H. Seo, E. Shin, S. H. Joo, O. Buyukcakir, Y. Jiang, M. Kim, H. Nam, S. K. Kwak and R. S. Ruoff, *Polym. Chem.*, 2022, **13**, 5309–5315.
23 Y. Jiang, H. Zhang, L. Hong, J. Shao, B. Zhang, J. Yu and S. Chu, *ChemSusChem*, 2023, **16**, e202300106.
24 L. Yao, J. King, D. Wu, S. S. C. Chuang and Z. Peng, *Catal. Commun.*, 2021, **150**, 106274.
25 M. Guláš, C. S. Cojocaru, F. Le Normand and S. Farhat, *Plasma Chem. Plasma Process.*, 2007, **28**, 123–146.
26 H. M. Nguyen, F. Gorky, S. Guthrie and M. L. Carreon, *Catal. Today*, 2023, **418**, 114141.